Crystal structure and magnetic properties of the unique Jahn-Teller system $^{154}Sm_{0.6}Sr_{0.4}MnO_3$

I. D. Luzyanin, V. A. Ryzhov, D. Yu. Chernyshov, A. I. Kurbakov, V. A. Trounov, A. V. Lazuta, V. P. Khavronin, I. Larionov, and S. M. Dunaevsky

Petersburg Nuclear Physics Institute, Gatchina 188350, St. Petersburg, Russia

(Received 5 June 2000; revised manuscript received 28 March 2001; published 14 August 2001)

Structural neutron diffraction investigations as well as data on resistance, linear susceptibility, and second harmonic of magnetization are presented for $^{154}Sm_{0.6}Sr_{0.4}MnO_3$ manganite. The structural studies reveal the unique Jahn-Teller (JT) character of this compound which is established to exhibit a *Pbmn* space group. Unusual large coherent JT distortions are found to develop below $T_{JT} \approx 180$ K and remain even in a metallic ferromagnetic phase below the Curie point $T_c \approx 120$ K. In the paramagnetic region the resistance is consistent with polaron hopping. A field hysteresis of the second harmonic is observed above T_c. This evidences the existence of the macroscopic ferromagnetic regions in the paramagnetic matrix. In contrast, temperature dependence of the linear susceptibility reveals a plateau at $T > T_c$. These conflicting peculiarities of the magnetic properties can be explained by assuming the ferromagnetic behavior to be associated with the antiferromagnetic regions possessing a weak ferromagnetism. The ordered regions appear as a result of first order transition at $T \approx 160$ K, destroy at $T_* \approx 137.5$ K and reveal a characteristic three-critical behavior for $T \to T_* + 0$. Change in a balance between the ferromagnetic double exchange hopping of e_g electrons and the antiferromagnetic interactions of t_{2g} spins, which caused by the cooperative JT effect, and the charge ordering correlations are supposed to account for the anomalous magnetic behavior above T_c.

DOI: 10.1103/PhysRevB.64.094432 PACS number(s): 75.40.Gb, 75.60.−d, 61.66.Fn

I. INTRODUCTION

Doped manganite perovskites have been extensively studied because of their interesting physics.[1] Some of these compounds reveal the colossal magnetoresistance properties. The $R_{1-x}Sr_xMnO_3$ (RSr) manganites with R=Sm belong to this group. Their magnetic phase diagram obtained by magnetic, transport, and electron diffraction measurements shows, in general, a rather typical behavior with increasing x.[2] Ferromagnetic insulating state, replacing antiferromagnetic insulating (AFI) phase, is found for $0.1 \leqslant x \leqslant 0.3$. For $0.3 < x < 0.52$, ferromagnetic metallic state is observed, an AFI phase occurs for $x > 0.6$, and these two ranges are sandwiched by an intermediate zone $0.4 \leqslant x \leqslant 0.6$, where the coexistence of the several phases are found. At the same time, the SmSr possesses a number of the peculiarities in a hole doped region ($x < 0.5$) distinguishing it even from the NdSr and PrSr compounds in which Nd^{3+} and Pr^{3+} radii are the nearest to that of Sm^{3+} and whose phase diagrams are the same character as that of SmSr in this area.[2,3] The first important feature is a low Curie temperature T_c which does not exceed 130 K for $x = 0.4$, whereas the maximum $T_c \approx 280$ K ($x \approx 0.4$) is found in the NdSr and PrSr. The most remarkable peculiarity is an unusual magnetic behavior above T_c for $x \leqslant 0.4$. In the paramagnetic state the data on a nonlinear response revealed the regions with a weak spontaneous magnetization for $x = 0.25$, 0.3, and 0.4.[4] A hysteresis of magnetization was also found in the relatively large magnetic fields for $x = 0.35$ above T_c which disappears at high temperatures.[5]

The manganites containing Sm have been poor studied by neutron diffraction due to a very large absorption cross section of natural Sm. In particular, there are no detailed data on the crystal structure of SmSr system which are of great importance for clarifying a role of the lattice effects. Only recently, character of a magnetic ordering below T_c for $x = 0.4$ has been established by neutron diffraction experiment.[6]

We report here the systematic investigations of $x = 0.4$ SmSr compound which include the structural neutron diffraction measurements as well as the data on resistivity, dynamic magnetic susceptibility, and nonlinear response. Our studies suggest that the very large cooperative Jahn-Teller (JT) distortions of $LaMnO_3$ type, which develop below $T_{JT} \approx 180$ K and only slightly reduce in the metallic ferromagnetic state below $T_c \approx 120$ K, underlie the peculiarities of this system.

We present evidence for the existence of the regions possessing a weak ferromagnetism (WF) in the paramagnetic phase. This property is attributed to the formation of *A*-type AF domains exhibiting the WF due to the Dzyaloshinskii-Moriya coupling. The ordered phase originates with a small finite magnetization below T_{JT} at $T \approx 160$ K, indicating a first order transition. Its nonlinear response is found to exhibit a strong enhancement at decreasing temperature, showing a three critical anomaly at $T_* \approx 137.5$ K where this ordered state completely destroys. Then at $T_c = 120$ K, the system undergoes transition into a new state which can be considered as a mixture of the charge-delocalized ferromagnetic and AFI phases. In addition, a small volume fraction of the *CE*-type AF phase is found to appear below T_{JT}, and persist down to 1.5 K without the noticeable temperature changes. Since the *CE* structure is associated with the charge ordering at $x \sim 0.5$, this observation is consistent with the findings of the work[2] where the local appearance of the charge ordering was found by electron diffraction below 140

K. In addition, these studies are in general agreement with our results on the coexistence of the several phases in this compound below T_{JT}. Note, that the several features of the magnetic behavior above T_c and a number of the structural peculiarities for our compound are similar to those of $(Nd_{1-y}Sm_y)_{0.5}Sr_{0.5}MnO_3$ $(y=0.94)$ (Ref. 7) and $Nd_{0.25}La_{0.25}Ca_{0.5}MnO_3$.[8]

Some preliminary data on the crystal structure and a character of magnetic ordering below T_c has been reported for this manganite earlier.[6] This work presents new data on Mn-O1(O2)-Mn bond angles, findings on a temperature hysteresis of the lattice constants, the more accurate results on Mn-O1(O2) bond lengths and evidence concerning the existence of the *CE*-type AF phase.

II. SAMPLE AND METHODS

The sample was prepared by multistage solid state synthesis from a stoichiometric mixture of MnO_2, $SrCO_3$, and Sm_2O_3 (using isotope ^{154}Sm) with intermediate grinding and pressing at 10 000 kg/cm^2. Synthesis was carry out into corundum crucible at 1200 °C for 48 h at one stage in air.

Sintered sample was certified for a content of the metal components, employing complexonometrical titration for determination of Sm, Mn with error $\leqslant 1\%$ and Sr with error $\leqslant 2\%$. The content of Sm was also determined photometrically. The correctness of this test was confirmed by an analysis of the artificial solutions and comparison of titration and photometry. Thus, the isotope powder sample of composition $^{154}Sm_{0.590(6)}Sr_{0.410(8)}Mn_{1.00(1)}O_3$ was prepared completely enriched with ^{154}Sm. The ^{154}Sm isotope has a rather small neutron absorption in comparison with a natural isotope mixture that allows us to perform the neutron diffraction experiments. According to our EPR data, there were no traces of the magnetic impurities in the sample. The magnetoresistivity was measured by the conventional four-probe method.

The neutron powder diffraction experiments on $^{154}Sm_{0.6}Sr_{0.4}MnO_3$ in a temperature range from 1.5 to 300 K were performed using G4.2 (LLB, France) high-resolution diffractometer. The program FULLPROF[9] was employed for the crystal structure refinement. A diffraction patterns at room temperature and at 1.5 K are shown in Fig. 1.

The dynamical linear susceptibility measurements were carried out by the same manner as in Ref. 10 in a frequency range 10^3–10^5 Hz; an ac field amplitude was $h_0 \approx 1$ Oe. A field hysteresis of the resistance and the susceptibility were studied in the weak constant magnetic fields $H \leqslant 500$ Oe.

The measurements of the second harmonic of the longitudinal component of magnetization M_2 were performed in parallel dc- and ac-harmonic magnetic fields $H + h \sin \omega t (h \leqslant 35$ Oe, $f = \omega/2\pi = 15.7$ MHz). The real and imaginary parts of the second harmonic of magnetization $\mathrm{Re}\, M_2(H)$ and $\mathrm{Im}\, M_2(H)$, were simultaneously recorded as the functions of the steady magnetic field H at various sample temperatures. This field was scanned symmetrically relative to the point $H=0$ for detecting a field hysteresis of the signal. An installation and a method of separation of the M_2-phase components have been described previously.[11] Sensitivity of this measurements was about 10^{-9} emu.

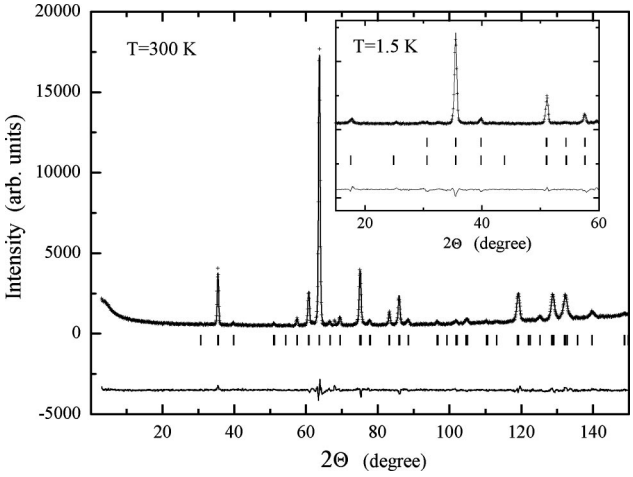

FIG. 1. Diffraction pattern, calculated profile, and residual curve for $Sm_{0.6}Sr_{0.4}MnO_3$ ($Pbnm$, room temperature). The inset shows the same for $T=1.5$ K. Magnitude of the residual curve is close to zero. It is placed below zero for convenience.

III. RESULTS AND DISCUSSION

A. Neutron diffraction data

Some details related to the diffraction experiments and the refinement procedure as well as the preliminary results have been reported earlier.[6] The measured diffraction profiles are found to be comparably well fitted by the orthorhombic space group $Pbnm$. The results on the lattice constants (Fig. 2) and MnO bond lengths $d_{\text{Mn-O}}$, (see Table I) show that $a = b > c/\sqrt{2}$ and all $d_{\text{Mn-O}}$ are equal (O phase) at $T = 180$ K–300 K. A remarkable splitting of the lattice constants a and b as well as the Mn-O distances develops below $T_{JT} \approx 180$ K ($O-O'$ structural transition). This typical coherent Jahn-Teller (JT) splitting is preserved down to 1.5 K. The lattice constants exhibit a temperature hysteresis in a large temperature range $T \approx 90$–175 K, that is due to a proximity of the two transitions of the first order: structural and metal insulator. A lattice response to the latter is clearly seen from the data obtained on heating, when the lattice distances display the kinks at $T \approx 90$ K with following nearly linear T

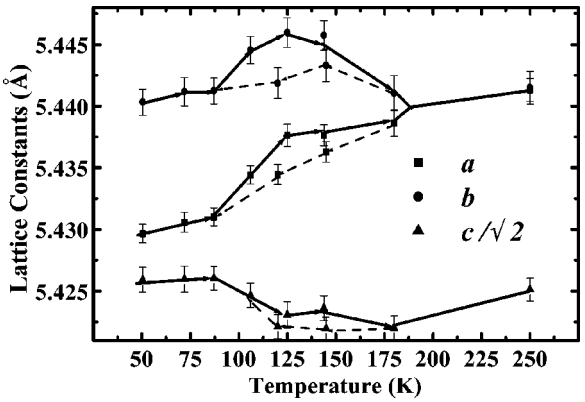

FIG. 2. Temperature dependencies of the lattice constants for $Sm_{0.6}Sr_{0.4}MnO_3$ ($Pbnm$) in heating and cooling regimes. The solid lines are a guide for the eyes.

TABLE I. Selected structural parameters for sample of $Sm_{0.6}Sr_{0.4}MnO_3$. All the refinements were carried out using the orthorhombic *Pbnm* space group. The numbers in parentheses are the statistical errors of the last significant digits.

T	*a*	*b*	*c*	Mn-O1	Mn-O2	Mn-O2	Mn-O2-Mn	Mn-O1-Mn
(K)	(Å)	(Å)	(Å)	(Å)	(Å)	(Å)	(deg)	(deg)
300	5.4415(6)	5.4419(9)	7.6730(7)	1.951(2)	1.96(2)	1.94(2)	160.0(2)	158.7(4)
144	5.4376(9)	5.446(1)	7.670(1)	1.938(2)	2.10(2)	1.81(2)	160.2(2)	163.3(5)
125	5.4376(9)	5.446(1)	7.669(1)	1.936(2)	2.12(2)	1.78(1)	160.3(1)	163.9(5)
106	5.4344(8)	5.445(1)	7.672(1)	1.937(2)	2.06(2)	1.86(2)	158.2(2)	163.8(5)
50	5.4297(8)	5.440(1)	7.673(1)	1.934(2)	2.07(2)	1.84(2)	157.8(2)	164.8(5)

dependencies up to $T_c \approx 120$ K. This behavior is in a close correspondence with that observed in $(Nd_{0.06}Sm_{0.94})_{1/2}Sr_{1/2}MnO_3$.[7] The lattice constants show the largest *T* hysteresis at T_c that reflects a peculiarity of the metal-insulator transition in the strong JT system. As seen from Table I, the equatorial (Mn-O2) bonds exhibit the abrupt changes, whereas an apical (Mn-O1) bond reveals the smallest variation across the JT transition as it occurs in $LaMnO_3$.[12] The cooperative JT distortions are also sensitive to metal-insulator transition. A difference between the two Mn-O2 bound lengths reduces from $\delta = 0.34(3)$ Å at $T \approx 125$ K ($\approx T_c$) to $\delta = 0.20(4)$ Å at $T \approx 106$ K. Surprisingly, the distortions of the MnO_6 octahedron in the metallic state are the same character as those in $LaMnO_3$,[12] namely, the Mn-O1 bond length lies between the Mn-O2 bond lengths. Moreover, $\delta \approx 0.2$ Å in this state is not far from $\delta \approx 0.3$ Å in the insulating state at $T \approx 144$ K which is nearly the same as δ in $LaMnO_3$.

Thus, the metallic ferromagnetic state of this compound reveals the unusually large coherent octahedral distortions. This is the new unexpected phenomenon for the doped manganites. Such a behavior may be related to adiabatic (above T_c) and nonadiabatic (below T_c) motions of the carriers.[13] An assumption of this scenario is that in the insulating state the mobility of the electrons is slow compared with the frequencies of the JT active phonons. If the $Mn^{3+}O_6/Mn^{4+}O_6$ octahedrons are fully distorted/undistorted in the insulating state, they relax completely during electron hopping from Mn^{3+} to Mn^{4+} site. In the metallic phase the carriers are more mobile and the octahedrons do not exhibit full relaxation. The local distortion of the $Mn^{3+}O_6$ octahedron may decrease in the metallic state, whereas the distortion of $Mn^{4+}O_6$ octahedron may increase, so that the average lattice structure reveals the strong distortions.

The bond angles, shown in Table I, also exhibit the temperature changes. The Mn-O1-Mn bond angle increases noticeably in the JT phase, compared to room temperature. The Mn-O2-Mn bond angle is sensitive to the insulator-metal transition displaying a reduction below T_c.

It is worth to present here the data on the magnetic structure below T_c partly reported earlier.[6] Neutron diffraction spectra at low temperatures reveals the ferromagnetic (F) and antiferromagnetic contributions. The F component is directed along the *c* axis. The AF component lying along the *b* axis orders ferromagnetically in the *ab* plane with AF alignment of the subsequent *ab* planes forming *A*-type AF structure. The F and AF reflections appear simultaneously below $T_c \approx 120$ K. The components of the magnetic moment per Mn site at 1.5 K are found to be $m_c = m_F = 2.46(5)\mu_B$ and $m_b = m_{AF} = 0.54(3)\mu_B$. These findings can be interpreted as evidence for the coexistence of the F and AF phases in this manganite since the so large predominance of the ferromagnetic component is unlikely can be provided by a stable AF state with the small m_{AF}. Indeed, hole doping in the manganites leads, as a rule, to the uniform F state at *x* less than $x = 0.4$. In this compound a corresponding value was found to be $x \approx 0.3$.[2] An alternative possibility, the homogeneous canted AF state with a comparably small ferromagnetic component, may occur at a low doping near a border between the AFI and ferromagnetic insulating phases where $x \sim 0.1$. The findings on this matter were reported, for instance, in Ref. 14 where $La_{1-x}Ca_xMnO_3$ with $x = 0.05$ and 0.08 was studied by neutron scattering.

A careful examination of the diffraction pattern reveals the small additional peaks corresponding to the *CE*-type AF ordering as Fig. 3 shows. This phase is observed below T_{JT}. Although the *CE*-type spin structure is characterized by two independent magnetic moments for Mn^{3+} and Mn^{4+} sites, their difference is within the statistical errors. The average magnetic moment of Mn ions lying along the *b* axis is found to be $m_{CE} = 0.31(2)\mu_B$ at 1.5 K.

At last, it is important to stress that the structural *Pbnm* model corresponds to an average diffraction pattern. The phases mentioned above are expected to be characterized by

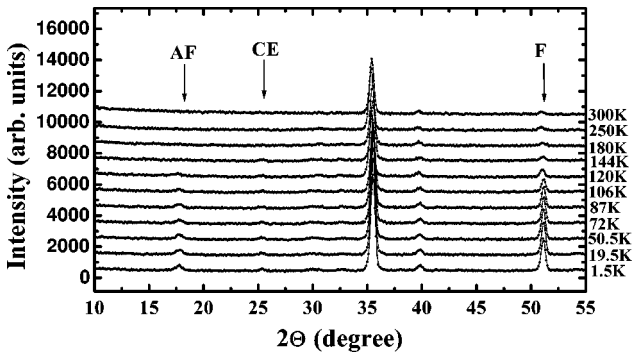

FIG. 3. Neutron diffraction spectra for different temperatures. The arrows indicate the changes corresponding to the antiferromagnetic, *CE*, and ferromagnetic phases.

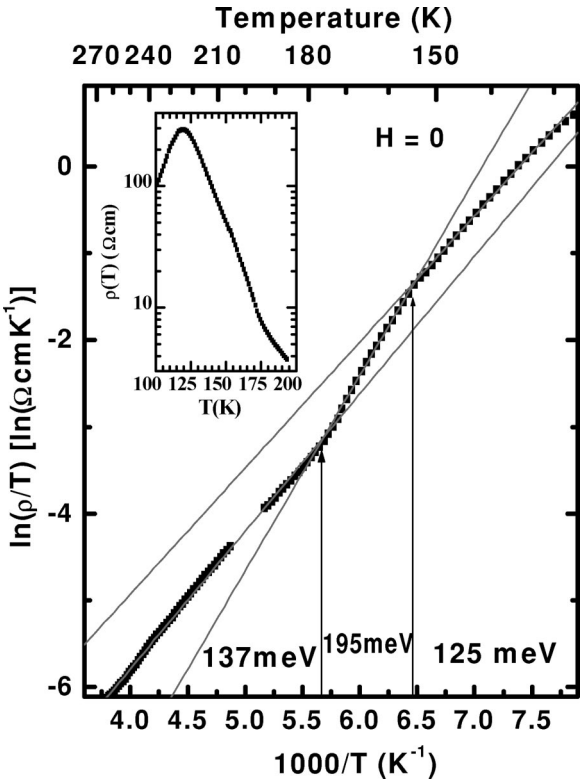

FIG. 4. Plot of $\ln(\rho/T)$ versus $1/T$ above T_c. The inset presents the dependence of ρ on T.

the different structural parameters. Consequently, a strong anisotropic broadening of the diffraction lines observed in this sample can be attributed to some distribution of the lattice constants. On the other hand, the relatively good fit of the diffraction pattern by this model suggests that these phases belong to the *Pbmn* space group and possess the comparably close structural parameters.

B. Resistance and linear magnetic susceptibility

Resistance $R(T)$ has a maximum at $T_m \approx 119$ K (see the inset in Fig. 3) with ratio $R(T_m)/R(300\ \mathrm{K}) \approx 10^3$. In the ferromagnetic phase it reveals metallic behavior down to a lower temperature border of the measurements (60 K). According to the data obtained in the magnetic fields varying from 100 to 500 Oe, $R(H)$ is practically linear function of H at T_m that is usually associated with the F state. The H hysteresis of the resistance is only observed below T_c. The $\ln(\rho/T)$ versus $1/T$ curve (Fig. 4), where ρ is the resistivity, shows three intervals of the linear dependencies above T_c that suggests polaronic character of the conductivity with the different hopping energies. Increase of the hopping energy below $T_{JT} \approx 180$ K may be associated with the coherent ordering of the distorted MnO_6 octahedra which leads to long-range polaron localization. A following reduction of this energy occurs below 160 K. Lack of any structural anomaly at this temperature suggests that this effect is probably caused by development of an AF ordered phase as the data on the nonlinear response given below show.

Temperature dependence of the linear susceptibility χ is measured at $H=0$ in a temperature range from 60 to 230 K

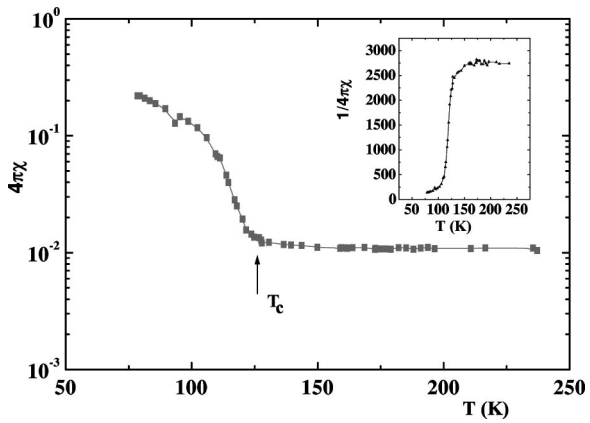

FIG. 5. The temperature dependence of $4\pi\chi'$. Insert shows the dependence of $1/4\pi\chi'$ versus T. The solid lines are a guide for the eyes.

(Fig. 5). The Curie point is defined as the temperature of sharp rise of χ (Ref. 15) that gives a value which approximately coincides with that obtained from neutron diffraction ($T_c \approx 120$ K). The imaginary part of the χ was rather weak and observed only at frequency 100 kHz. It is worth to point out that a H hysteresis of linear susceptibility is found only below T_c as for the resistance.

In the paramagnetic region, χ is practically independent of T between 130 and 240 K. This can be interpreted as an effect of short range AF fluctuations developing at these temperatures. The plateau in $\chi(T)$ appears above T_{JT} that can be explained by influence of the short range charge-ordering correlations which promote the *CE*-type AF ordering.[7,8] Then, below T_{JT}, the JT effects come into play intensifying significantly the tendency to the antiferromagnetism so that the AF ordered regions appear at $T \approx 160$ K. Such unusual peculiarities are a consequence of the cooperative JT effect which controls a relationship between the ferromagnetic double exchange and the AF superexchange coupling of t_{2g} spins. This effect is driving mechanism for orbital ordering which in turn influences strongly, first of all, e_g-electron hopping.[16] The latter accounts for the one-electron band width and, consequently, the double exchange arising from itinerancy of the doped holes. The AF couplings are not expected to be modified so strongly by the JT ordering. Thus, the decrease in T_c and the unconventional character of the magnetic behavior above T_c can be attributed to the reduction in the double exchange caused by the coherent JT effect and the charge-ordering correlations. Note that in the manganites with $x \sim 0.5$ a relationship between the charge and magnetic correlations seems to persist up to very high temperatures.[17]

C. Second harmonic of magnetization

The measurements of the second harmonic of magnetization M_2, is performed in a temperature range from 135 to 230 K. $\mathrm{Re}\, M_2$ is only detected, no $\mathrm{Im}\, M_2$ is found. We observe a field hysteresis up to 160 K which is much higher than T_c, the signal being found at $H=0$. $\mathrm{Re}\, M_2(T)$ reduces monotonically as temperature increases so that the accurate

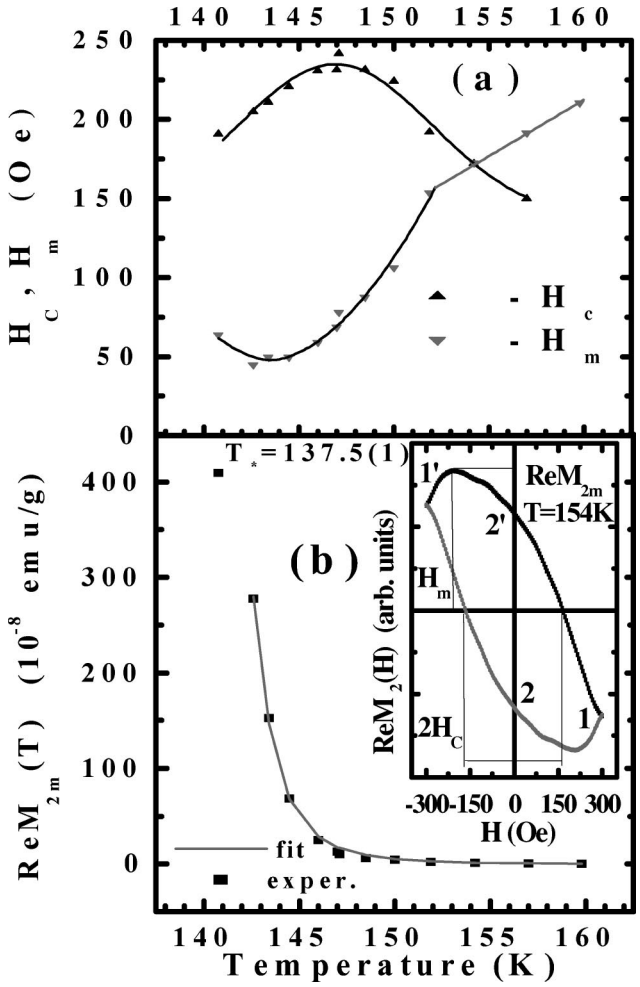

FIG. 6. The temperature dependence of the $\mathrm{Re}\,M_2$ parameters. Panel (a) presents data on the coercive field H_C and the position H_m of the $\mathrm{Re}\,M_2(H)$ extremum. Panel (b) does it for the extremum value $\mathrm{Re}\,M_{2m}$ of the $\mathrm{Re}\,M_2(H)$. The inset in panel (b) shows a typical dependence of the $\mathrm{Re}\,M_2$ on H. The solid lines in panel (a) are a guide for the eyes. The solid line in panel (b) presents the fit of the experimental dependence of the $\mathrm{Re}\,M_{2m}(T)$ in a range $T=142.6$ K–160 K which is described in the text.

measurements are impossible above 160 K. Below 140 K a magnitude of the signal increases sharply and a strong suppression of a radio frequency power is needed to record the response without saturation. At the same time, at low level of the power we could not register correctly the phase components of the signal. Therefore, our possibilities for an analysis of the data were limited by the temperature range above 135 K. The typical hysteresis loop at $T\approx 154$ K is presented in the insert of Fig. 6(b). We characterize these hysteresis loops by means of (i) a maximal value of $\mathrm{Re}\,M_2(H)$; (ii) the positions of this maximum H_m; (iii) M_{2m} coercivity, H_c. Figures 5(a), 5(b) present these quantities as the functions of temperature.

The existence of the response at $H=0$ provides clear evidence of a spontaneous magnetization M_{sp} of a sample. Indeed, M_2 is a pseudovector and an even function of h. Therefore, $M_2(H)$ is odd in H with $M_2(0)=0$ in the paramagnetic phase. Consequently, this signal is very sensitive to the appearance of M_{sp}, because in this case $M_2\neq 0$ at $H=0$.[18] In the present study, the slowly scanned H forms the quasistatic hysteresis loop of magnetization M with a remanent magnetization M_r and a coercive field. The high frequency $h(t)$ perturbs weakly this state that leads to M_2 generation which reveals the hysteresis as a function of H with $M_2(0)\propto \pm M_r$.

We concentrate first on a magnetic type of a phase which can possess M_{sp}. The M_{sp} found in the insulating state can be attributed to the AF ordered regions with a WF component due to small Dzyaloshinskii-Moriya coupling. This interpretation agrees with the main peculiarities of the data. First of all, it allows us to clarify a relationship between $\chi(T)$ behavior and the occurrence of the ferromagnetism above T_c. According to the argumentation given above, the plateau in $\chi(T)$ is related to the development of the AF correlations throughout the sample that is sufficient to modify the typical T dependence of χ above T_c. In addition, a part of the sample can exhibit the long-range AF ordering. As it will be seen, this ordering is not so easy to be observed by neutron diffraction. At the same time, the WF due to Dzyaloshinskii-Moriya coupling is often too small to be detected by χ measurements used here. For instance, the nonlinear response evidenced such a WF associated with a phase separation of extra oxygen in $La_2CuO_{4+\delta}$, whereas the χ measurements failed to reveal it.[19]

We believe that the WF is related to the *A*-type AF state since the orthorhombic $c/\sqrt{2}$ axis is the shortest one for this structure,[3] and, namely, such an AF phase can coexist with the F state below T_c, with a volume fraction being compatible with that of the F phase. The *CE*-type charge ordered AF state can also occurs for the observed crystal structure.[3] However, a similar nonlinear response was found in SmSr manganites with $x=0.3$ and $x=0.25$ (Ref. 4) that cannot be connected to any charge ordering. At the same time, the very weak reflections, which can be attributed to the *CE*-type state, are observed in the neutron diffraction pattern for $x=0.4$. This phase appears below T_{JT} and persists down to 1.5 K exhibiting no noticeable temperature changes. These observations correlate with the appearance of an extremely weak M_2 signal at $T\approx 170$ K which is distinguishable from that presented above. It reveals another H dependence showing a maximum at a small $H_m\approx 61$ Oe, its position and maximum magnitude being practically independent on temperature. There is no such a signal in the SmSr compounds with $x=0.25$ and 0.3.[4] These fundings suggest that the *CE* phase cannot account for the WF.

It is interesting to compare the properties of our compound with those of $Nd_{1-x}Sr_xMnO_3$ for $x=0.49$ and 0.51 which display the *Ibmm* crystal structure below 400 K.[3] This space group is very close to the *Pbnm*. The essential difference between them is coincidence of two Mn-O bond lengths in the *ab* plane for the *Ibmm* symmetry. In the NdSr ($x=0.4$) manganite a metallic F ordered state, which develops below $T_c=280$ K, coexists with *CE*-type AF structure below $T_N^{CE}\approx 160$ K, the *CE* phase dominating at 15 K. With decreasing temperature, the $x=0.51$ sample exhibits the F transition at $T_c\approx 240$ K, then *A*-type AF ordering develops

below $T_N^A \approx 200$ K, and the *CE*-type appears at $T < T_N^{CE} \approx 150$ K. In this case the F, *A* and *CE*-type AF phases coexist in narrow temperature range below T_N^{CE}. At $T = 10$ K only *A* and *CE* structures are observed, the *A*-type dominating.

In our sample the ''incipient'' AF ordering definitely appearing below T_{JT} is taken over by the F state below T_c, so that at low temperature AF phase coexists with the F phase, the later dominating. A small amount ($\leqslant 10\%$) of the *CE*-type AF phase, which is observed at $T < T_{JT}$, also presents in the ground state.

The comparison shows that the coexistence of the three magnetic structures (F, *A*, and *CE*) for $x \sim 0.5$ is the common feature of these systems exhibiting the *Pbnm* and *Ibmm* symmetries. The combination of these phases, their relative volume fractions and the temperature regions in which they occur depend on the level of doping and the space group. For instance, the *CE* phase reduces in our system compared to NdSr. As important differences between the NdSr system and our manganite we note that, first, in the former the spins are ordered along the longest *b* axis (in our notations) for all the types of manganite ordering, whereas in our sample ferromagnetic moment is directed along *c* axis. Second, our manganite shows another character of changes of the lattice constants at the magnetic ordering in addition to the strong coherent JT distortion in the *ab* plane.

We consider now the peculiarities of the *A*-type AF regions which can lead to the WF. $LaMnO_3$ is the reasonable reference point. In this system the WF is due to the Dzyaloshinskii-Moriya interaction of the nearest Mn^{3+} spins $\mathbf{S}_i$ and $\mathbf{S}_j$ in the adjacent ferromagnetic planes $\mathbf{d}_{ij}[\mathbf{S}_i \times \mathbf{S}_j]$, where $\mathbf{d}_{ij} = (d_a, d_b, 0)$ for some fixed *i* and *j*, and direction of $\mathbf{d}_{ij}$ is determined by the tilting of the MnO_6 octahedron.[20–22] For the ferromagnetic moments of two neighboring *ab* planes, $\mathbf{M}_{1,2}$, oriented along *b* axis with AF mutual alignment, we get the WF magnetization along *c* axis: $M_c \approx (J_{bc}/J_\perp)L_b$ for $J_{bc}/J \ll 1$. Here $\mathbf{L} = (\mathbf{M}_1 - \mathbf{M}_2)/2$ is the staggered magnetization, $J_{bc} = d_a$ and $J_\perp$ is the AF isotropic superexchange of the neighboring Mn^{3+} spins in the adjacent planes. The magnetization of the planes is directed along the longest crystalline axis (*b* in our notation) in all the manganites exhibiting the *A*-type AF state in *Pbnm* structure[3] that suggests the same orientation in our case. For $LaMnO_3$, this is due to the JT distortions of MnO_6 octahedron which gives rise to the dominating single ion anisotropy along the longest Mn-O bond.[12,22] This factor is likely to be responsible for the anisotropy of the doped compounds too. For the same direction of **L**, coincidence of the tilting pattern of the MnO_6 octahedron leads to that of their canted AF states.

The close qualitative resemblance of the crystal structure of these systems and the same type of the magnetic ordering may be thought to provide a similar magnetic behavior. Considering the nonlinear response of these magnets, one should take into account the peculiarities of our measurements and data. The former suggests that $M_2 \propto h^2$ and, according to the results, $\mathrm{Im}\, M_2(\omega, H)$ is not observed in the present manganite. When $M_2 \propto h^2$, the response can be written as $M_2(\omega, H) \propto \chi_2(\omega, H) h^2$, where χ_2 is the susceptibility of second order which has a static limit $\chi_2(0,H) = \mathrm{Re}\, \chi_2(0,H) = 1/2 \partial^2 M/\partial H^2$, whereas $\mathrm{Im}\, \chi_2(0,H) = 0$.[18] The inequality $|\mathrm{Im}\, \chi_2(\omega)/\mathrm{Re}\, \chi_2(\omega)| \equiv r(\omega) \ll 1$ means at low ω that $\mathrm{Re}\, \chi_2(\omega, H) \approx \mathrm{Re}\, \chi_2(0,H)$ is detected. This is, in fact, a consequence of the general properties of the susceptibilities and can be checked for χ_2 using a simple relaxation approximation in which $r(\omega) \propto \omega/\Gamma$ at $\omega/\Gamma \ll 1$, where Γ is the relaxation rate of *M*.[18,19] Thus, it is enough to elucidate a reason of nonlinearity of $M(H)$ to understand the M_2 generation.

Since magnetization data in a steady *H* and measurements of ac susceptibility have revealed an anisotropic critical behavior of monocrystalline $LaMnO_3$,[22] the noticeable nonlinearity in this system is expected to occur in the vicinity of T_N for *H* directed along the *c* axis. As will be seen in detail below, the Dzyaloshinskii-Moriya interaction connecting L_b and M_c leads to influence of H_c on L_b. The L_b, as a critical variable, exhibits a nonlinear *H* dependence in a relatively small *H* that, in turn, gives rise to a nonlinearity of $M_c(H)$. The nonlinear response will reveal a critical enhancement above T_N with $M_2 \propto H$ for $H \to 0$. Below T_N, $M_2(H)$ has to show a field hysteresis with $M_2 \neq 0$ at $H = 0$. The M_2 generation will be anisotropic, the major effect being found along the *c* axis.

Note that the response with the above characteristic properties was observed in $La_2CuO_{4+\delta}$ single crystals.[19] The peculiarities of a distribution of extra oxygen made it possible to relate the M_2 generation to a nonlinear critical behavior of a CuO_2 plane with uncompensated WF. Using this assumption, the *H* dependence of $\chi_2(\omega, H)$ was described quantitatively in the paramagnetic critical region, the nonlinearity of $M(H)$ being, in fact, the reason of the M_2 generation.

The response of the present manganite, however, reveals no the traces of the paramagnetic behavior because the M_2 generation is accompanied by the *H* hysteresis. This indicates that the phase accounting for the response appears by a jump, as a result of first-order transition at $T \approx 160$ K $< T_{JT} \approx 180$ *K*, when the JT distortions reach a definite level. Then, at decreasing *T*, the signal shows a strong enhancement below $T \approx 150$ K [Fig. 6(b)]. This behavior suggests a critical anomaly related to destabilization of the ordering.

Analyzing this transition, we employ a mean-field theory. Since the present AF phase has the same symmetry as that of $LaMnO_3$, one can use a free energy Φ for the latter[23] with an usual additional term to allow first-order transition. For the two relevant variables describing the ordering, the staggered magnetization L_b and magnetization M_c, the Φ reduces to a two sublattice expression which for $\mathbf{H} \| \mathbf{c}$ is written as

$$\Phi = 1/2 A L_b^2 + 1/4 B L_b^4 + 1/6 P L_b^6 - D_{bc} L_b M_c + 1/2 \chi_0^{-1} M_c^2 - M_c H. \quad (1)$$

In the case of $LaMnO_3$ exhibiting the second order transition, A, B and χ_0 are determined by the exchange interactions $P = 0$ and D_{bc} introduces the Dzyloshinskii-Moriya coupling. If L_b and M_c are measured in the units of $g\mu_B$ per Mn, $A(T) \sim T_N \tau$, $\tau = (T - T_N)/T_N$, $B \sim \chi_0^{-1} \sim T_N$, and $D_{bc} \sim J_{bc}$, where $T_N = 140$ K and $J_{bc} \approx 0.4$ K.[12,22]

The sixth-order term in Eq. (1) allows one to describe the first-order transition which can occur for negative B. The modification of the transition is a result of the complicated relationships between spin, lattice, orbital, and charge degrees of freedom. Since this transition occurs during development of the structural transition, the JT effects are most likely to play a leading role in it.

Now, minimizing Φ, we get

$$AL+BL^3+PL^5=\tilde{H}, \tag{2}$$

$$\tilde{H}=dH, \quad d=D\chi_0,$$

$$M=\chi_0 H+dL. \tag{3}$$

Here the axes indices have been omitted. We have employed $A-D^2\chi_0\approx A$ in Eq. (2) because an easy-axis anisotropy $J_{\rm an}\geqslant J_{bc}$ has been included in A and $J_{\rm an}\geqslant J_{bc}D\chi_0$, where $D\chi_0=d\ll 1$ is the usual small parameter for the WF.

According to Eqs. (2),(3), the appearance of a spontaneous $L_{\rm sp}$ at $H=0$ generates $M_{\rm sp}=dL_{\rm sp}$. For $H\neq 0$, they determine $M(H)$, with a nonlinearity of $L(H)$ leading to that of $M(H)$.

Consider the first-order transition. For $H=0$, a free energy corresponding to Eq. (2) is given by Eq. (1) at $M_c=0$, and we obtain $\Phi(L)$ with a well known phase diagram characterized by the parameters A and B.[24] The first-order transition occurs in a region $A>0$ and $B<0$ when $-B$ reaches a value $-B=4(PA/3)^{1/2}$ determined from the conditions $\Phi(L)=0$ and $\partial\Phi/\partial L=0$. This relation between B and A gives a line of the diagram where two phases with $L=0$ and $L_{\rm sp}^2=-3B/4P$ are in an equilibrium to each other; for $B^2>16PA/3$ the ordered phase dominates.

In the magnetic state Eqs. (2),(3) give for $H\to+0$

$$M_{\rm sp}=dL_{\rm sp}=d[-B+(B^2-4AP)^{1/2}]^{1/2}, \tag{4}$$

with $B^2\geqslant 16PA/3$.

Let us turn to behavior of $L(H)$ and $M(H)$ in the ordered phase. It is clear, that these functions exhibit the jumps from $-L_{\rm sp}(-M_{\rm sp})$ to $L_{\rm sp}(M_{\rm sp})$ at $H=0$ when H varies from $H_-<0$ to $H_+>0$. At the same time, $\partial L/\partial H$ and susceptibility χ determined from Eqs. (2),(3)

$$\frac{\partial L(H)}{\partial H}=d[A+3BL^2(H)+5PL^4(H)]^{-1}, \tag{5}$$

$$\chi(H)=\frac{\partial M(H)}{\partial H}=\chi_0+d\frac{\partial L(H)}{\partial H}=\chi_0+\chi_{\rm WF}(H), \tag{6}$$

are the continuous functions of L^2 and, consequently, H. It can be checked that $\partial L/\partial H$ is finite and $\partial L/\partial H>0$. The $\chi_{\rm WF}$ in Eq. (6) is the WF component of the susceptibility. The Eqs. (5),(6) give

$$\chi_2(H)=\frac{1}{2}\frac{\partial^2 M(H,\tau)}{\partial H^2}$$

$$=-L(H)[10PL^2(H)+3B]\left(\frac{\partial L(H)}{\partial H}\right)^3. \tag{7}$$

The $\chi_2(H)$ has a discontinuity $\triangle\chi_2\propto L_{\rm sp}=M_{\rm sp}/d$ in going across $H=0$. It can be verified that $\partial\chi_2(H)/\partial H>0$.

The H behavior of this system characterized by the functions $M(H),\chi(H)$, and $\chi_2(H)$ is qualitatively the same as that of a weak ferromagnet or a ferromagnet below second order transition. However, T behavior of these magnets can be quite different. According to our data, M_2 increases sharply with decreasing T. We will show that Eq. (7) for χ_2 can describe this effect if $A(T)$ and $B(T)$ tend to zero simultaneously for $T\to T_*$ where T_* is the three-critical point.[24] On the contrary, the magnets exhibiting second-order transition cannot reveal such a behavior in an ordered phase.

Considering T dependence of χ_2, we employ a generally accepted suggestion in the mean field theory: $B(T)\propto\tau=(T-T_*)/T_*$ for $T\to T_*+0$. Parameter A can be assumed to vary as $A\propto\tau^q$ with $q=2$ to satisfy inequality $B^2\geqslant 16PA/3$. If $q>2$, this coefficient becomes unessential near T_*. It is convenient to introduce a parametrization: $-B/P=b\tau$, $4A/P=\tilde{a}\tau^2$, and $\tilde{a}/b^2=a(a\leqslant 3/4$ from the above inequality), where b, $\tilde{a}$ and a are the dimensionless coefficients as L and M are measured in the units of $g\mu_B$ per Mn. This system of the units will be also used below.

In the introduced notations Eqs. (4),(5) yield

$$M_{\rm sp}(\tau)=dL_{\rm sp}(\tau)=dC_{\rm sp}b^{1/2}\tau^{1/2}, \tag{8}$$

$$C_{\rm sp}=[1+(1-a)^{1/2}]^{1/2}/\sqrt{2};$$

$$\left.\frac{\partial L}{\partial H}\right|_{H=0}=C_{L'}dP^{-1}b^{-2}\tau^{-2}, \tag{9}$$

$$C_{L'}=\{[1+(1-a)^{1/2}](1-a)^{1/2}\}^{-1}.$$

We present $\chi_2(H,\tau)$ in a weak $H\geqslant 0$ which is deduced from Eqs. (7)–(9)

$$\chi_2(H,\tau)=\chi_2(\tau)\left(1-C_\delta\frac{dH}{P(\tau b)^{5/2}}\right)=\chi_2(\tau)[1-\delta\chi_2(H,\tau)], \tag{10}$$

$$C_\delta=6C_{L'}\left[C_{\rm sp}^2C_0^2C_{L'}-\left(1+\frac{5}{4}(1-a)^{1/2}\right)\right](C_{\rm sp}C_0)^{-1};$$

$$\chi_2(\tau)=-C_{\chi_2}d^3P^{-2}(\tau b)^{-9/2},$$

$$C_{\chi_2}=C_{\rm sp}C_{L'}^3C_0, \quad C_0=2\left(1+\frac{5}{2}(1-a)^{1/2}\right). \tag{11}$$

In this regime L induced by H, $L\sim\tilde{H}/P(b\tau)^2$ Eq. (9), is much less than $L_{\rm sp}\sim(b\tau)^{1/2}$ so that $\tilde{H}/P(b\tau)^{5/2}\ll 1$ in Eq. (10). In a strong H as $\tilde{H}/P(b\tau)^{5/2}\gg 1$, χ_2 is mainly deter-

mined by H: $\chi_2 \propto H^{-9/5}$. At last, we give an expression for $M_2(\tau)$ at $H \to +0$ which is obtained from Eqs. (8),(11)

$$M_2(\tau) = -C_{M_2} M_{\rm sp}(\tau) \left(\frac{dh}{P(b\tau)^{5/2}} \right)^2, \qquad C_{M_2} = C_L^3, C_0 . \tag{12}$$

As should be expected, the magnitude of M_2 is reduced by the weak-field factor in square in comparison with $M_{\rm sp}$. The coefficients $C_{\rm sp}, C_\delta$, and C_{χ_2} in Eqs. (8), (10), (11) vary with a as follows. The factor $C_{\rm sp}$ reduces weakly from 1 to $\sqrt{3}/2$ when a increases from zero to 3/4. The same change of a leads to monotonous increasing C_{χ_2} from 7/8 to 9.23 and C_δ from 8.6 to 35.

The parameter a controls a distance from the border of the first order transition determined by the condition $a = 3/4$. Equation (8) shows that b accounts for the magnitudes of $L_{\rm sp}$ and $M_{\rm sp}$. A value of $L_{\rm sp}$ at saturation given formally by Eq. (8) at $\tau = 1$ restricts that of b: $C_{\rm sp} b^{1/2} \leqslant S_0$, where $S_0 = 1.7$ for a mixture of Mn^{3+} and Mn^{4+} ionic states corresponding to our manganite with $x = 0.4$. The parameter P determines the scale of the magnetic field effect on L and M as it is clear from Eqs. (9), (10), (12). Since three critical behavior is not effected by interaction of the fluctuations,[24] the obtained results can be directly compared with the experimental data.

Although there is not any deep physical sense in a comparison of the three critical indices with those of the second order transitions in the 3D isotropic magnets, it seems useful to do it. The $M_{\rm sp}$ and $L_{\rm sp}$ scale as $(T - T_*)^\beta$ with $\beta = 1/2$ Eq. (8) so that this index coincides with that of the mean field results for $M_{\rm sp}$ (F-paramagnet transition, $T \to T_c - 0$) or $L_{\rm sp}$ (AF-paramagnet transition, $T \to T_N - 0$). Note that scaling theory gives $\beta \approx 1/3$ for these transitions.[24] An index γ of a staggered susceptibility determined by Eq. (9) and $\chi_{\rm WF}$ Eq. (6) is $\gamma = 2$, whereas scaling prediction is $\gamma \approx 4/3$ for the compared systems. At last, a magnetic field H_{cr} dividing the regimes of the weak and strong fields obeys a law $H_{cr} \propto \tau^{\beta+\gamma}$ with $\beta + \gamma = 5/2$ and $\beta + \gamma \approx 5/3$ for our case and 3D isotropic magnets, respectively.

Let us proceed to the experimental findings. In a real magnet the steplike $M_2(H)$ dependence transforms into a hysteresis curve due to domain formation. One can compare the $\chi_2(H,\tau)$ dependencies with behavior of the branches (1-2) and (1′-2′) of $\mathrm{Re}\, M_2(H)$ hysteresis loop displayed in the inset of Fig. 6. These branches can only reveal the dependencies which may be similar to those obtained for the uniform state. The (1-2) branch shows a minimum whose absolute value sharply increases at decreasing T, its field position H_m monotonically decreasing from 200 Oe down approximately to 50 Oe. This behavior is similar to that expected in the weak H, where $M_2 \propto \tau^{-4.5}$ Eqs. (10),(11). According to Eq. (10), $M_2(H)$ has to increase with raising H. In our case, however, it occurs for $H > H_m$. This peculiarity may be understood if H_m is the border for formation of the near-uniform state. In the weak ferromagnets, in contrast to the conventional ones, so homogeneous state can be provided by a relatively weak H in virtue of the small magnitudes of $M_{\rm sp}$ and susceptibility, the latter remaining not too large even near T_* as following estimations show.

Thus, the T dependence of M_{2m} can be compared with the prediction $M_2(\tau) \propto \tau^{-\gamma_2}$ with $\gamma_2 = 9/2$ for $T \to T_*$. Figure 6(b) shows, that this expression fits well the $M_{2m}(T)$ data, with a fitting three critical temperature T_* being found to be $T_* \approx 137.5(2)$ K. Note that the fit of the data at $H = 0$ gives practically the same T_* with a close value of mean-squared deviation of the data to the fit. Thus, heterogeneity of the magnetic state in a range between $H = 0$ and H_m is not so significant to modify the temperature dependence of M_2. It is worth indicating that the fit of $M_{2m}(T)$ data including the two relevant parameters T_* and γ_2 gives $T_* = 134.5(9)$ K and $\gamma_2 = 6.7(5)$. Although the formal result of this kind cannot be interpreted unequivocally, it seems to support indirectly the presence of the three critical anomaly at $T_* \approx 137.5$ K since the sinqularity in this point gives the value of $\gamma_2 = 4.5$ which is physically justified and maximal close to that obtained in the two parametric treatment.

In the vicinity of T_* at $T \approx 140.8$ K, the response in a field region $0 < H < H_m \approx 64$ Oe is about five times less than M_2 calculated from the expression obtained in the fit. Since in this interval $M_2(H)$ depends very weakly on H, this effect cannot be attributed to the H influence and means change in the critical behavior which manifests itself in a very strong suppression of $M_{\rm sp}$ and, consequently, $L_{\rm sp}$. Modification of the temperature dependencies of the critical variables in the close proximity of a critical temperature is known phenomena which usually occurs in a region of τ where some weak interactions become strong enough.[24] In the present phase a corresponding coupling is most likely to be the interaction between the fluctuations of M and L which is, in fact, controlled by a parameter $(d/\tau)^2$ and becomes strong as $\chi_{\rm WF} \propto (d/\tau)^2$ Eqs. (6),(9) exceeds χ_0. The estimations given further confirm this assumption. The additional careful investigations are certainly needed to elucidate the peculiarities of the critical behavior in this narrow temperature region just above T_*. Thus, the presented theory describes well the T dependence of M_2 in a large range of changing $M_2(T)$, about three orders of magnitude, using the single relevant fitting parameter T_*.

Now consider the parameters P, d, and b. Since each of them cannot be determined from the data, we first set $P = T_*$ that is the natural assumption in the critical region. From Eqs. (11),(12) with a correction on an angle averaging needed for the polycrystalline magnets and the data on $\mathrm{Re}\, M_{2m}$ obtained at $h \approx 35$ Oe, we find a relation $[f_{\rm WF} C_{\chi_2}(a)]^{1/3} d/b^{3/2} \approx 4 \times 10^{-2}$ where $f_{\rm WF}$ is the volume fraction of the sample occupied by the ordered phase. This expression, however, is insufficient to estimate the parameters of the phase. An additional relationship between b and d can be obtained by using the influence of H on M_2 given by Eq. (10). Introducing the quantities

$$m_2 = |M_2| P^2 \tau^{9/2}/h^2 = C_{\chi_2} f_{\rm WF} d^3/b^{9/2}, \tag{13}$$

[see Eqs. (8),(11),(12)] and

$$\delta\tilde{\chi}_2 = \delta\chi_2 (P\tau^{5/2}/H) = C_\delta d/b^{5/2} \tag{14}$$

[see Eq. (10)], we get

$$d = C_d \left(\frac{m_2}{f_{\mathrm{WF}}} \right)^{5/6} \delta\tilde{\chi}_2^{-3/2}, \qquad C_d = C_\delta^{3/2} / C_{\chi_2}^{5/6}; \tag{15}$$

$$\tilde{C}_{\mathrm{sp}} = C_{\mathrm{sp}} b^{1/2} = C_{\mathrm{sp}}^* \left[\left(\frac{m_2}{f_{\mathrm{WF}}} \right)^{1/3} \delta\tilde{\chi}_2^{-1} \right]^{1/2}, \qquad C_{\mathrm{sp}}^* = C_{\mathrm{sp}} (C_\delta / C_{\chi_2}^{1/3})^{1/2}. \tag{16}$$

Here we present coefficient $\tilde{C}_{\mathrm{sp}}$ determining the full magnetization of the material $L_{\mathrm{sp}} = \tilde{C}_{\mathrm{sp}} \tau^{1/2}$ Eq. (8). A remarkable peculiarity of Eqs. (15),(16) is that the coefficients C_d and $\tilde{C}_{\mathrm{sp}}$, unlike C_{χ_2} and C_δ, change weakly with a; at increasing a from 0 to 3/4, they increase slightly: C_d from 30.5 to 32.5 and $\tilde{C}_{\mathrm{sp}}$ from 3 to 3.5. An angle averaging, which should be made for a polycrystalline magnet, leads to replacement $M_2 \rightarrow 4M_2$ in Eq. (13) and $\delta\chi_2 \rightarrow 5/4\delta\chi_2$ in Eq. (14) since $M_2 \propto h^2$ at $H=0$ and $\delta M_2 = \delta\chi_2 h^2 \propto H h^2$. As it was mentioned, the H effect described by Eq. (10) is modified by influence of the domain structure. An examination of $M_2(H)$ dependence shows that this influence reduces with decreasing T but, nevertheless, exists even at the minimal available $T=142.6$ K. Therefore, one can only obtain an estimation $\delta\chi_2 \leqslant 0.2$ at $T=142.6$ K and $H=100$ Oe. As a result, Eqs. (15),(16) give $d \geqslant 1.8\times10^{-2}/f_{\mathrm{WF}}^{5/6}$ and $\tilde{C}_{\mathrm{sp}} \geqslant 0.8/f_{\mathrm{WF}}^{1/3}$. If a considerable part of the sample is ordered, for instance $f_{\mathrm{WF}} = 0.5$, we find $d \geqslant 3.2\times10^{-2}$ and $\tilde{C}_{\mathrm{sp}} \geqslant 1$. The values of $d \approx 3.2\times10^{-2}$ is close to $d \approx 4.5\times10^{-2}$ of $LaMnO_3$ (Ref. 22) that seems to be reasonable for the systems with nearly the same JT distortions. The value of $\tilde{C}_{\mathrm{sp}} \approx 1$ corresponds to about 60% of the fully magnetized phase ($L_{\mathrm{sp}} \approx \tau^{1/2} \approx 0.6 S_0 \tau^{1/2}, S_0 = 1.7$) if factor $\tau^{1/2}$ is ignored. This reduction appears to be rather natural for the phase which originates at the finite T due to the interactions of spin degrees of freedom with other ones. In contrast, if $f_{\mathrm{WF}}=0.1$, we get $d \geqslant 12\times10^{-2}$ and $\tilde{C}_{\mathrm{sp}} \geqslant 1.7$. The so large d and maximal allowed $\tilde{C}_{\mathrm{sp}}$ suggest that this situation is unlikely to occur.

Thus, according to the estimations, the large volume fraction of the sample is expected to exhibit the ordering. For definiteness, the possible parameters of the phase can be $f_{\mathrm{WF}} \sim 0.5$, $d \sim 3\times10^{-2}$ and $\tilde{C}_{\mathrm{sp}} \sim 1$. This conclusion does not contradict the neutron diffraction data and χ measurements. Indeed, a relative magnetization per Mn is $\delta L_{\mathrm{sp}} = L_{\mathrm{sp}}/S_0$ with $S_0 = 1.7$. For 50% ordered sample with $\tilde{C}_{\mathrm{sp}} \approx 1$, we have $\delta L_{\mathrm{sp}} \approx 0.5 \tilde{C}_{\mathrm{sp}} \tau^{1/2}/S_0 \approx 0.1$ at $T=160$ K. This result shows that it is not so easy to reveal the AF peaks of the relatively small intensity which, in addition, unexpectedly quickly disappear with decreasing temperature.

As regards to χ exhibiting the plateau in the considering temperature range where $4\pi\chi = 10^{-2}$ (Fig. 5), the WF contribution to it is small besides a close vicinity of T_* because the critical enhancement is compensated by the smallness of d, $\chi_{\mathrm{WF}} \propto (d/\tau)^2$ Eqs. (6),(9). Calculation of maximal $\delta\chi_{\mathrm{WF}} = \chi_{\mathrm{WF}}/3\chi$ (1/3 is a result of averaging) for the chosen parameters gives $\delta\chi_{\mathrm{WF}} \approx 2.7\times10^{-3}$ at $T=160$ K and $\delta\chi_{\mathrm{WF}} \approx 0.1$ at $T=141$ K where the maximal $C_{L'}/b^2 \approx 0.75$ has been used.

It is interesting to compare χ of the sample and χ_0 of our phase. There are two different susceptibilities in the ordered phase: $\chi_\perp$ and $\chi_\parallel$ measured perpendicular and along L_{sp} correspondingly. In an above expressions χ_0 is $\chi_\perp$. The $\chi_\perp$, being independent of T in AF state, coincides with its paramagnetic limit at T_N. Exploiting the single energy scale of our problem T_*, χ_0 can be presented as $\chi_0 = C[(g\mu)^2/a_0^3]T_*^{-1}$ (the conventional units), where $a_0 \approx 3.8$ Å is the structural constant of the pseudocubic lattice of the manganite and C is the numerical factor. It gives $4\pi\chi_0 = 0.64\times10^{-2}$ compared to $4\pi\chi = 10^{-2}$ of the sample, if $C = S(S+1)/3 = 1.55$ is simply the paramagnetic factor for the mixture of Mn^{3+} and Mn^{4+} ionic states corresponding to $x=0.4$. Since L_{sp} is small, $\chi_\parallel$ is expected to be close to $\chi_\perp$ and, therefore, the both components of the susceptibility of the phase are comparable to χ of the sample. This means that the phase can occupy a considerable part of the sample, in agreement with above conclusion.

At last, spin-flop transition, which occurs in this phase for $\mathbf{H} \| \mathbf{L}_{\mathrm{sp}}$, is characterized by spin-flop field H_{SF}. This field can be roughly estimated as $g\mu H_{\mathrm{SF}} \sim (T_* J_{\mathrm{an}})^{1/2} \tau^{1/2}$ where we employ $\chi_0 = \chi_\perp \propto T_*^{-1}$ and $\tau^{1/2}$ determines the reduction of L_{sp}. It gives $H_{\mathrm{SF}} \approx 5$ at 160 K and 1.5 T at $T=140$ K if $J_{\mathrm{an}} \approx 2$ K as in $LaMnO_3$.[22] This evaluation excludes the spin flop as a possible reason of the M_2 generation in so weak H used in our study. Note that the close values of H_{SF} were observed in the similar manganite $(Nd_{0.06}Sm_{0.94})_{1/2}Sr_{1/2}MnO_3$, H_{sp} reducing with decreasing T.[7] These findings support correctness of our analysis.

Consider briefly the (2′-1) and (2-1′) branches of the loop in the inset of Fig. 6 which appear due to domain formation. The M_2 generation here is mainly related to domain-wall motion. A characteristic scale of this nonlinearity is determined by the coercive field H_c which shows a smooth T dependence displayed in Fig. 6(a). The corresponding nonlinear behavior was considered on the basis of the simplest one dimension model of a nonlinear oscillator describing the domain-wall vibrations within the pinning wells.[25] This dynamics will not be analyzed here.

The unusual magnetic behavior above T_c suggests an unconventional type of the phase transition in this system at T_c. In a temperature range between T_c and T_*, the AF fluctuations are most likely to remain great and, at the same time, the F fluctuations grow at $T \rightarrow T_c + 0$, so that one may expect a strong interaction between them. This can effect the transport properties, especially the magnetoresistance, and may lead to the new peculiarities of insulator-metal transition.

IV. CONCLUSION

The structural neutron diffraction study on $Sm_{0.6}Sr_{0.4}MnO_3$ powder sample shown that in this system the strong coherent JT distortions developed below T_{JT}

≈ 180 K and remained even in the FM phase. This structural ordering modifies the transport and magnetic properties in the paramagnetic phase above $T_c \approx 120$ K. The transport measurements revealed the polaron character of conductivity above T_c with the hopping energy which increases sharply below T_{JT}. The $\chi(T)$ exhibited the unusual plateau above T_c, and the nonlinear response indicated the appearance of regions possessing the spontaneous magnetization below 160 K. The latter phenomenon is attributed to the formation of the *A*-type AF domains with the WF due to the Dzyaloshinskii-Moriya interaction. The ordered regions were found to appear by a jump at $T \approx 160$ K and gave the response with the characteristic temperature dependence which suggests the three critical anomaly at $T \approx 137.5$ K corresponding to destruction of the ordering. The volume fraction of this phase, its magnetization and AF order parameter were estimated. In addition, the small amount of the *CE*-type AF phase was found below T_{JT} by neutron diffraction measurements. These magnetic data evidence the dominant character of the AF and, to a lesser extent, charge fluctuations between T_c and T_{JT}. This phenomenon is explained by changing in the subtle balance between the ferromagnetic double exchange and the AF interactions of t_{2g} spins caused by the cooperative JT effect. The definite orbital ordering due to this effect is assumed to lead to a reduction of the effective e_g hopping that favors the AF peculiarities in the magnetic behavior. Note that the short range charge ordering fluctuations in this manganite are expected to develop above T_{TJ}, at least, at $T \sim 230$ K where we start to observe the plateau in $\chi(T)$.

A role of the cooperative JT effect in physics of the manganites is not well understood even in the case of the undoped compounds since the strong Coulomb interaction can produce the similar influence on the ground state. Some of the theoretical works have stressed the importance of the coherent JT distortions,[16,21,26] whereas a conclusion on the dominant effect of the electronic mechanism has been made in other studies.[27,28] For the doped manganites situation is more complicated. The materials exhibiting the metal-insulator transition show typically collapse of the cooperative JT distortions as it occurs in $La_{1-x}Sr_xMnO_3$ for $x > 0.16$.[29] Some aspects of this phenomenon have been analyzed in work (Ref. 30). Although the Coulomb interaction is undoubtedly important in the compounds with $x \sim 0.5$ which reveal no the coherent JT effect,[31] another scenario can take place in the opposite case. It has been recently shown that a strong coupling between electron and JT phonon systems can stabilize the charge ordering for $x = 0.5$, with the competing F and *A*-type AF states also appearing in the calculations.[32] The presented compound is expected to be an important example of this type.

ACKNOWLEDGMENTS

The authors would like to thank A.P. Nechitailov and A.A. Nechitailov for the sample preparation and I.A. Kiselev for assistance in the nonlinear response measurements. The neutron diffraction experiment was supported by the State Program of Neutron Investigations (NI). We also acknowledge the support of the Russian Foundation for Basic Research (Grant Nos. 00-02-16729 and 00-02-81205 Bel2000_a) in the magnetic and transport investigations.

[1] *Colossal Magnetoresistance, Charge Ordering and Related Properties of Manganese Oxides*, edited by B. Raveau and C. N. R. Rao (World Scientific, Singapore, 1998).
[2] C. Martin, A. Maignan, M. Hervieu, and B. Raveau, Phys. Rev. B **60**, 12 191 (1999).
[3] R. Kajimoto, H. Yoshizawa, H. Kawano, H. Kuwahara, Y. Tokura, K. Ohoyama, and M. Ohashi, Phys. Rev. B **60**, 9506 (1999).
[4] I.D. Luzyanin, V.A. Ryzhov, S.M. Dunaevsky, V.P. Khavronin, I.I. Larionov, A.V. Lazuta, and Yu.P. Chernenkov, Fiz. Tverd. Tela **42**, 290 (2000) [Phys. Solid State **42**, 298 (2000)].
[5] R.P. Borges, F. Ott, R.M. Thomas, V. Skumryev, J.M.D. Coey, J.I. Arnaudas, and L. Ranno, Phys. Rev. B **60**, 12 847 (1999).
[6] D.Yu. Chernyshov, V.A. Trounov, A.I. Kurbakov, S.M. Dunaevsky, and J. Rodriguez-Carvajal, Mater. Sci. Forum **321-324**, 812 (1999).
[7] H. Kuwahara, Y. Moritomo, Y. Tomioka, A. Asamitsu, M. Kasai, R. Kumai, and Y. Tokura, Phys. Rev. B **56**, 9386 (1997).
[8] A. Arulraj, A. Biswas, A.K. Raychaudhuri, N.C.R. Rao, P.M. Woodward, T. Vogt, D.E. Cox, and A.K. Cheetham, Phys. Rev. B **57**, R8115 (1998).
[9] J. Rodrigues-Carvajal, Physica B **192**, 55 (1993).
[10] I.D. Luzyanin and V.P. Khavronin, Zh. Éksp. Teor. Fiz. **85**, 1029 (1983) [Sov. Phys. JETP **58**, 599 (1983)].
[11] G.K. Anisimov, R.P. Devyaterikov, E.I. Zavatskii, V.V. Lavrov, V.A. Ryzhov, D.M. Fel'dman, and V.N. Fomichev, Zh. Tekh. Fiz. **52**, 74 (1982) [Sov. Phys. Tech. Phys. **27**, 46 (1982)].
[12] J. Rodrigues-Carvajal, M. Hennion, F. Moussa, A.H. Moudden, L. Pinsard, and A. Revcolevschi, Phys. Rev. B **57**, R3189 (1998).
[13] M. Medarde, J.F. Mitchell, J.E. Millburn, S. Short, and J.D. Jorgensen, Phys. Rev. Lett. **83**, 1223 (1999).
[14] F. Moussa, M. Hennion, G. Biotteau, J. Rodriguez-Carvajal, L. Pinsard, and A. Revcolevschi, Phys. Rev. B **60**, 12 299 (1999).
[15] A. Maignan, C. Martin, F. Damay, and B. Raveau, Phys. Rev. B **58**, 2758 (1998).
[16] D. Feinberg, P. Germain, M. Grilli, and G. Seibold, Phys. Rev. B **57**, R5583 (1998).
[17] K.H. Kim, M. Uehara, and S-W. Cheong, Phys. Rev. B **62**, R11 945 (2000).
[18] A.V. Lazuta, I.I. Larionov, and V.A. Ryzhov, Zh. Éksp. Teor. Fiz. **100**, 1964 (1991) [Sov. Phys. JETP **73**, 1086 (1991)].
[19] A.V. Lazuta, V.A. Ryzhov, I.I. Larionov, and T.I. Arbuzova, Physica C **295**, 22 (1998).
[20] G. Matsumoto, J. Phys. Soc. Jpn. **29**, 606 (1970).
[21] I. Solovyev, N. Hamada, and K. Terakura, Phys. Rev. Lett. **76**, 4825 (1996).
[22] V. Skumryev, F. Ott, J.M.D. Coey, A. Anane, J.-P. Renard, L. Pinsard-Gaudard, and A. Revcolevschi, Eur. Phys. J. B **11**, 401 (1999).

[23] Fan Zhong and Z.D. Wang, Phys. Rev. B **60**, 11 883 (1999).
[24] A. Z. Patashinskii and V. L. Pokrovskii, *Fluctuation Theory of Phase Transitions* (Pergamon, Oxford, 1980).
[25] L.B. Rozenbaum, Fiz. Tverd. Tela (Leningrad) **12**, 2503 (1970).
[26] W.Y. Hu, M.C. Qian, Q.Q. Zheng, H.Q. Lin, and H.K. Wong, Phys. Rev. B **61**, 1223 (2000).
[27] K.I. Kugel' and D.I. Khomskii, Zh. Éksp. Teor. Fiz. **64**, 1429 (1973) [Sov. Phys. JETP **37**, 725 (1973)].
[28] L.F. Feiner and A.M. Oleš, Phys. Rev. B **59**, 3295 (1999).
[29] B. Dabrowski, X. Xiong, Z. Bukovski, R. Dybzinski, P.W. Klamut, J.E. Siewenie, O. Chmaissem, J. Shaffer, C.W. Kimball, J.D. Jorgensen, and S. Short, Phys. Rev. B **60**, 7006 (1999).
[30] Y. Motome and M. Imada, Phys. Rev. B **60**, 7921 (1999).
[31] R. Maezono, S. Ishihara, and N. Nagaosa, Phys. Rev. B **58**, 11 583 (1998).
[32] S. Yunoki, T. Hotta, and E. Dagotto, Phys. Rev. Lett. **84**, 3714 (2000).